Appl. Phys. A 72, 361–365 (2001) / Digital Object Identifier (DOI) 10.1007/s003390000534

Applied Physics A
Materials
Science & Processing

Angular-dependent photoemission studies of indium tin oxide surfaces

W. Song[1,2], **S.K. So**[1,*], **L. Cao**[2]

[1] Department of Physics and Centre for Surface Analysis and Research, Hong Kong Baptist University, Kowloon Tong, Hong Kong, P.R. China
[2] Department of Chemistry, Tsinghua University, Beijing, 100084, P.R. China

Received: 7 February 2000/Accepted: 28 March 2000/Published online: 13 September 2000 –

Abstract. Indium tin oxide (ITO) surfaces were treated by solvent cleaning, by plasma of oxygen, argon, nitrogen and by argon ion (Ar^+) sputtering. Angular-dependent X-ray photoelectron spectroscopy (ADXPS) and ultraviolet photoelectron spectroscopy (UPS) were used to determine the chemical composition, the chemical states and the work function after each treatment. It was found that oxygen plasma and nitrogen plasma chemically reacted with the ITO surfaces. Yet little etching of the surface can be observed after plasma treatments. Among all treatments, oxygen-plasma-treated ITO achieved the highest work function of 4.40 eV, whereas Ar^+-sputtered ITO surface had the lowest work function of 3.90 eV. The stoichiometry of the ITO surface is shown to be the major controlling factor of the ITO work function.

PACS: 81.65.Cf; 68.55.Nq

Indium tin oxide (ITO) is widely used as the anode material for organic light emitting devices (OLEDs) because of its high transparency and low resistivity [1, 2]. As a hole-injecting electrode, the surface properties and the work function of ITO directly affect the efficiency of carrier injection into organic layers. When used without some type of surface treatments, the devices fabricated with ITO usually exhibit poor device performance [3, 4]. It has been known that oxygen plasma treatment or ultraviolet-ozone treatment of ITO before the fabrication of OLEDs can significantly improve the device efficiency, brightness and reliability [5, 6]. Several studies focused on the relation between ITO surface treatments and its surface properties in order to clarify the effect of ITO surface treatments [7–11]. Most of them correlated the work function of ITO and its surface chemical composition. In our earlier paper we discussed the removal of carbon contamination on ITO surfaces treated by UV-ozone and its effects on OLEDs' performance [7]. Mason et al. reported that the work function of ITO is largely determined by the surface oxygen concentration [10]. Sugiyama et al. reported that three factors: (i) C-containing contaminants, (ii) the O/In ratio, and (iii) the In/Sn ratio on the ITO surface affected the work function [11]. In this work, angle-dependent X-ray photoelectron spectroscopy (ADXPS) and ultraviolet photoelectron spectroscopy (UPS) were employed to analyze the chemical composition, the chemical states and the work function of ITO before and after different surface treatments, including solvent cleaning, oxygen, argon, nitrogen plasma treatments and Ar^+ sputtering.

*Corresponding author. (E-mail: skso@hkbu.edu.hk)

1 Experimental

ITO thin films on glass substrates were purchased from Sanyo Vacuum Industries. They have a thickness of 1500 Å and a sheet resistance of 11.4 Ω/□. ITO thin films were first cleaned by scrubbing in detergent and then in distilled water.

Then they were immersed sequentially in ultrasonic baths of ethanol and acetone, each for about 15 min. Then they were blown dry in a clean hood. Plasma treatments were carried out using a PLASMA-PREEN system. Plasma was generated by microwave in an atmosphere of oxygen, argon, or nitrogen excitation at a pressure of 5 psi and a flow rate of 2.0 scfh. After plasma treatment or solvent cleaning, the samples were transferred into ultrahigh vacuum as soon as possible.

XPS and UPS measurements were performed using a VG-CLAM+4LH multichannel hemispherical analyzer. The analysis chamber was maintained at 2×10^{-7} Pa during XPS measurement, 6×10^{-6} Pa during UPS measurement due to He, and 5×10^{-5} Pa during Ar^+ sputtering due to Ar backfilling. The XPS spectra were recorded using an achromatic Al K_α excitation (1486.6 eV), with a power of 200 W and a pass energy of 20 eV. ADXPS measurements were carried out both at 90° and 15° take-off angle (TOA, relative to the sample surface). The surface sensitivity was significantly enhanced using a low TOA as shown in Table 1 [12, 13]. The UPS spectra were recorded using a VG UPS/2 Source, He I radiation ($h\nu = 21.22$ eV) from an unfiltered, windowless gas

Table 1. Information depth of XPS at different take-off angles

Take-off angle	Information depth (Å)	Reference
90°	~ 80	[12, 13]
15°	~ 20	

discharge lamp, with a pass energy of 2 eV. The work function Φ was determined by the following relation:

$$\Phi = h\nu - \Delta E$$

where ΔE is the energy, difference between the Fermi level and the secondary electron cutoff [14]. The sample was biased at -4.0 eV during UPS in order to observe the low-energy secondary cutoff. The position of the Fermi level was determined using silver as a reference.

2 Results and discussion

2.1 Changes in atomic concentrations under different surface treatments

Figure 1 shows the atomic concentrations of ITO surfaces recorded under different treatments at 15° and 90° TOA. Comparing to 90° TOA, the signal of C 1*s* at 15° TOA is significantly higher under each treatment. This indicates that a thin layer of carbon contamination remains at the ITO surface after each treatment. Oxygen plasma treatment resulted in the highest oxygen concentration at the surface. A small amount of nitrogen (1.5% of atomic concentration ratio) was observed after nitrogen plasma treatment. Thus, both O-plasma and N-plasma treatments could independently introduce oxygen and nitrogen to the ITO surface.

Table 2 shows the indium-to-tin ratio after different treatments. Similar ratios were obtained after solvent cleaning and oxygen plasma treatments: in both cases In:Sn was about 9 : 1 at 90° TOA, and 7 : 1 at 15° TOA. (The ratio was slightly larger for argon and nitrogen plasma treatments.) Hence plasma treatments do not etch much of the surface layer. This ratio turned into about 19 : 1 both at 90° and 15° TOA after 3 min of Ar^+ sputtering. So after sputtering the concentration of In increased, while the concentration of Sn decreased. The Sn enrichment at ITO surface is a common phenomenon, and is related to the migration of Sn-rich phases to the surface [15].

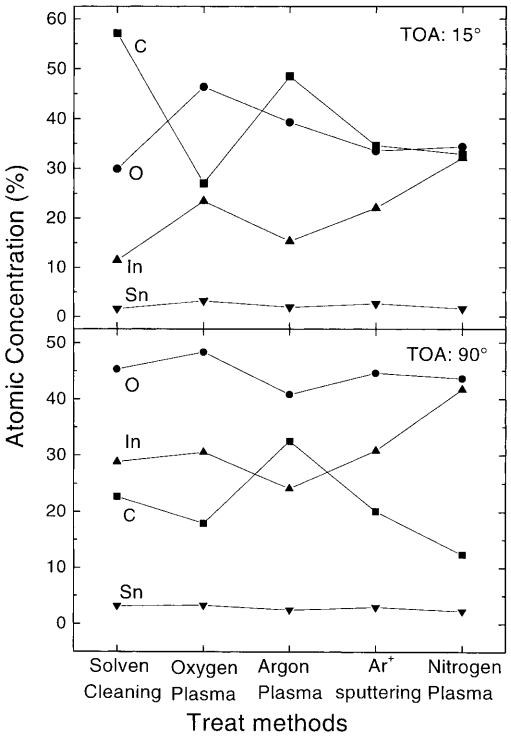

Fig. 1. Changes in atomic concentrations of ITO under different surface treatments

2.2 The removal of carbon contamination

Figure 2 shows one of the curve-fitting results for the C 1*s* orbital. Two kinds of carbon signals can be distinguished from the C 1*s* spectra: C−H at 285.0 eV and C−O at 288.0 eV. Table 3 shows the curve-fitting results of C 1*s* orbital under different treatments. It is clear that O-plasma and N-plasma can greatly reduce the hydrocarbon and the C−O contamination at the surface. However argon plasma treatment shows

Table 2. The indium-to-tin ratio after different treatments

	Solvent cleaning	Oxygen plasma	Argon plasma	Nitrogen plasma	Sputtering
In:Sn at 90° TOA	9.0	9.1	9.5	10.4	18.4
In:Sn at 15° TOA	6.9	7.3	8.2	8.4	19

Table 3. Variation of carbon atomic concentration using different treatment methods

Methods	Carbon atomic concentration			
	90° TOA		15° TOA	
	Hydrocarbon	C−O	Hydrocarbon	C−O
Solvent cleaning	18.2%	4.3%	48.9%	8.2%
Oxygen plasma	15.5%	2.4%	23.1%	3.9%
Nitrogen plasma	17.1%	3.0%	29.5%	5.1%
Argon plasma	27.6%	4.9%	40.7%	7.8%
Ar^+ sputtering	11.6%	0.9%	29.4%	3.4%

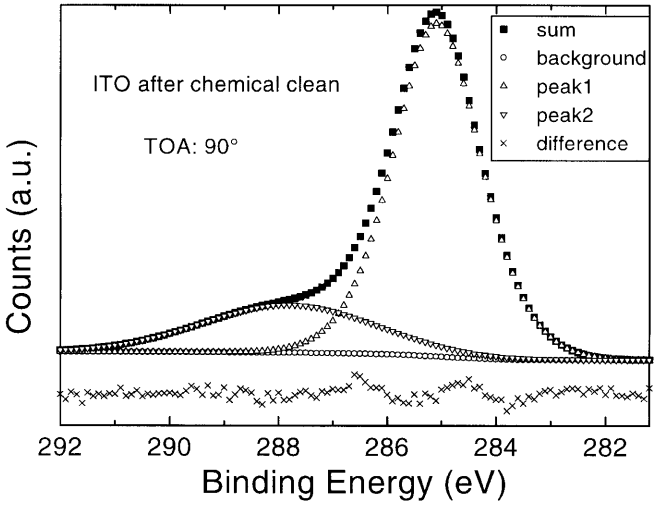

Fig. 2. A typical curve-fit result for C 1*s* orbital

poor results. Residual carbon signals after O-plasma and N-plasma treatments are probably introduced during sample transfer from air to UHV. There was still 12.5% of carbon at 90° TOA after 3 min of Ar^+ sputtering. This result suggests that part of the carbon may originate from the ITO bulk.

2.3 The peak position and full width at half maximum (FWHM) of In $3d_{5/2}$

Figure 3 showed the In 3*d* peaks after different treatments. The peak position of In $3d_{5/2}$ was independent of treatment conditions and remained constant at 444.7 eV under 90° TOA and 444.8 eV under 15° TOA. The FWHM of In $3d_{5/2}$ was determined to be 1.99 eV at 90° TOA and 2.10 eV at 15° TOA after solvent cleaning. This remained unchanged after argon plasma treatment. After oxygen plasma treatment, the FWHM of In $3d_{5/2}$ changed into 1.97 eV and 2.07 eV at 90° and 15° TOA (not shown). This was most probably caused by oxidation of the ITO surface. The change in the In $3d_{5/2}$ peak was relatively large after N-plasma treatment. The FWHM of In $3d_{5/2}$ increased to be 2.03 eV at 90° TOA and 2.13 eV at 15° TOA, which was probably caused by the chemical reaction between nitrogen and indium. As mentioned before, N 1*s* peak located at 400.3 eV can be observed after N-plasma treatment, which confirmed the existence of the chemical reaction between indium and nitrogen.

For solvent-cleaned, O-plasma and N-plasma treated surfaces, the FWHM of In $3d_{5/2}$ at 15° TOA is 0.1 eV larger than at 90° TOA. This indicated that the chemical states of indium at the top layer of ITO thin films are more complicated than in the bulk of ITO. After sputtering, the FWHM of the In $3d_{5/2}$ peak changed to 1.89 eV at 90° TOA and 1.91 eV at 15° TOA, and its shape became more symmetric. Indium in ITO bulk mainly exists in the lattice of In_2O_3. Our results show that indium at ITO surface exists in a more complex form than in the ITO bulk.

2.4 The peak position and FWHM of Sn $3d_{5/2}$

Figure 4 shows the peak position and FWHM of Sn $3d_{5/2}$ orbital after solvent cleaning and Ar^+ sputtering. Using the same XPS system, the peak position and FWHM of Sn $3d_{5/2}$ in SnO_2 were also independently determined to be 487.0 eV and 1.70 eV, respectively. The FWHM of Sn $3d_{5/2}$ in ITO after each treatment remained unchanged at about 2.14 eV both at 90° and 15° TOA. The relatively broad Sn 3*d* peak in ITO suggested that Sn in ITO exists in a much more complex form than Sn in bulk SnO_2. In ITO, Sn mainly enters substitutionally in the cation sublattice and acts as an n-type donor.

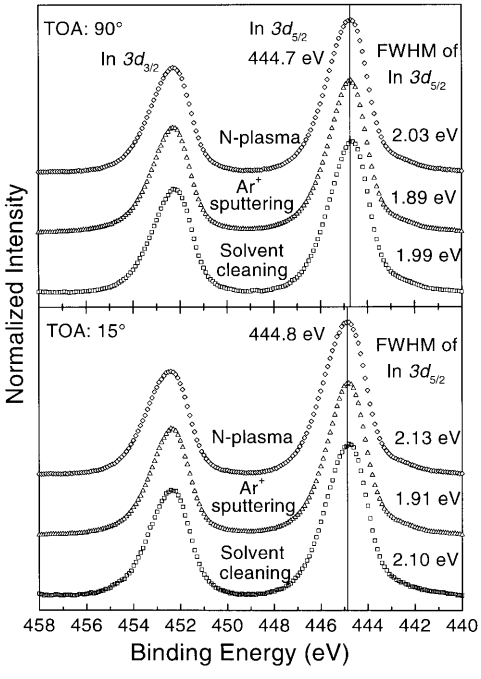

Fig. 3. In 3*d* spectra after solvent cleaning (□); Ar^+ sputtering (Δ); and N-plasma (◇)

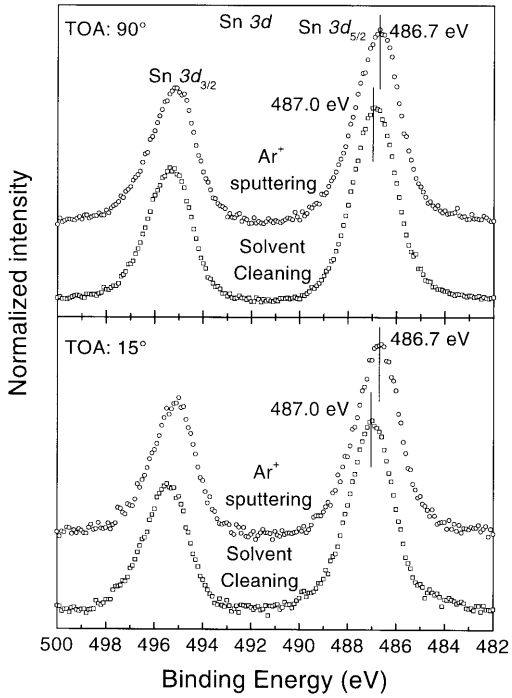

Fig. 4. Sn 3*d* spectra after solvent cleaning (□) and Ar^+ sputtering (○)

However, some defects, such as $(Sn_2O_4)^x$, were formed during ITO preparation [16]. The peak position of Sn $3d_{5/2}$ after solvent cleaning (Fig. 4) and plasma treatments (not shown) remained at 487.0 eV, which indicated that Sn at ITO surface mainly existed in the form of Sn^{4+}. The binding energy of Sn $3d_{5/2}$ shifted to 486.7 eV after sputtering, which indicated that the main component of Sn after sputtering changed into a lower oxide state, such as Sn^{3+} or Sn^{2+}. The change of chemical state of Sn after sputtering was probably caused by the selective sputtering of oxygen [17].

2.5 Analysis of O 1*s peak after different treatments*

The O 1*s* peak of ITO was fitted by three components centered at 530.3 ± 0.1 eV, 531.5 ± 0.1 eV, and 532.8 ± 0.1 eV, respectively. Figure 5 showed a sample of O 1*s* curve-fitting results (after solvent cleaning). The component centered at 530.3 eV can be assigned to O^{2-} ions in the tetrahedral interstices of face-centered-cubic In^{3+} ion array [18]. The component at 532.8 eV is due to loosely bound O^0 from contamination. The medium binding energy component centered at 531.5 eV has two contributors: (1) oxygen from C−O contamination, and (2) oxygen bound to In and Sn in ITO. This state is the intermediate state between O^{2-} and dissociated oxygen. Its electron density is smaller than the O^{2-} ions. The oxygen atomic concentration of C−O contamination can be obtained from the curve-fit results of C 1*s* (Table 3). If the components centered at 531.5 eV and 530.3 eV were added together and the concentration of oxygen from C−O contamination (from Table 3) was subtracted, then the concentration of oxygen bound to In and Sn can be obtained. This was labeled as $[O_{InSn}]$. In order to obtain the stoichiometry of ITO thin films, the $[O_{InSn}]/1.5[In] + 2[Sn]$ atomic concentration ratios after different treatments were calculated and are shown in Table 4. Oxygen plasma treatment achieved the highest $[O_{InSn}]/1.5[In] + 2[Sn]$ atomic concentration ratio especially at 15° TOA. This indicates that oxygen plasma treatment improves the stoichiometry of ITO surfaces especially at the top layers. Oxygen plasma not only removed the surface carbon contamination, but also chemically reacted with ITO surface layers. The $[O_{InSn}]/1.5[In] + 2[Sn]$ atomic concentration ratio was relatively small after sputtering. This proved the selective sputtering of oxygen by Ar^+ bombondment [17].

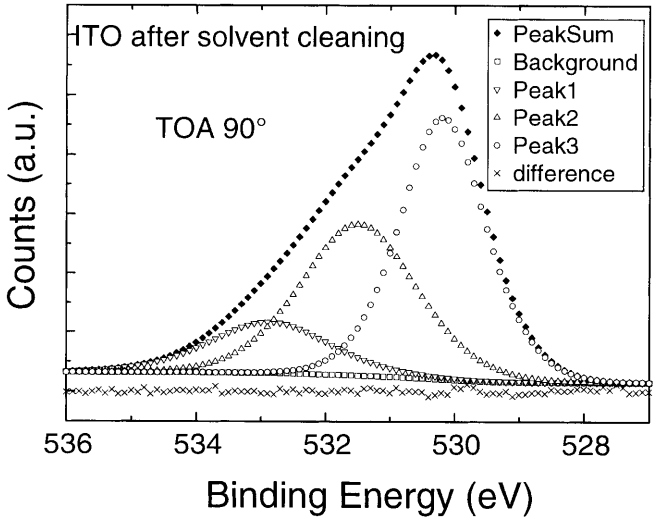

Fig. 5. A typical curve-fit result of ○ 1*s* orbital

2.6 Work function changes under different treatment methods

The work functions of ITO thin films after different treatments are shown in the last column of Table 4. Oxygen plasma treatment achieved the highest work function of 4.40 eV. This result is in good agreement with Nüesch et al. [8]. From Table 4, we can deduce the two factors that can affect the work function: (i) carbon contamination on ITO surface, (ii) the stoichiometry of ITO. ITO can be considered to be stoichiometric if the ratio of $[O_{InSn}]/1.5[In] + 2[Sn]$ is high. First let us discuss the effect of carbon contamination. Oxygen and nitrogen plasma treatments can remove most of the hydrocarbon contamination of ITO surface and result in an ultimate work function of 4.3–4.4 eV. Therefore, O-plasma and N-plasma can enhance the work function of ITO by removing carbon contamination. The work function after Ar-plasma treatment was also 0.1 eV higher than after solvent cleaning, and yet, in this case, no significant removal of carbon contamination from ITO surface can be observed. Hence, surface carbon contamination has a relatively small effect on the work function. Second, the best stoichiometry for ITO surface was obtained when ITO was treated with O-plasma. Concomitantly, the highest work function of 4.40 eV was achieved. Thus the stoichiometry of ITO should be the main factor that controls the work function of ITO. After sputtering, the work function was 0.50 eV lower than after oxygen-plasma treatment. Correspondingly, the $[O_{InSn}]/1.5[In] + 2[Sn]$ ratio was also much lower.

3 Conclusions

ITO thin films were treated by solvent cleaning, by plasma of oxygen, argon, and nitrogen, and by Ar^+ sputtering. The major results and conclusions are summarized below:

Table 4. Comparing the chemistry and work function of ITO after various treatments

Treatment	Carbon removal	$[O_{InSn}]/1.5[In] + 2[Sn]$ 90° TOA	15° TOA	Work function (eV)
Solvent cleaning	No	0.70	0.64	4.15
Oxygen plasma	Yes	0.75	0.76	4.40
Argon plasma	No	0.72	0.62	4.26
Nitrogen plasma	Yes	0.72	0.68	4.32
Ar^+ sputtering	Yes	0.64	0.59	3.90

(i) ADXPS indicates that ITO surface is Sn-rich, and In on ITO surface exists in more complex chemical states than in the bulk. For solvent cleaning and plasma treatments, Sn at ITO surface exists mainly in the form of Sn^{4+}. A reduction reaction occurred during Ar^{+} sputtering.

(ii) Both oxygen plasma and nitrogen plasma are effective in removing surface hydrocarbons from ITO surfaces. Correspondingly, argon plasma shows poor effect. Little etching of the ITO surface can be observed after plasma treatments.

(iii) Oxygen-plasma treatment increases the surface oxygen concentration of ITO. A small amount of nitride appears after nitrogen plasma treatment. Both oxygen and nitrogen plasma treatments could independently introduce oxygen and nitrogen to the ITO surface.

(iv) Two factors can affect the work function of ITO: (a) surface carbon contamination and (b) the surface stoichiometry of ITO. In general, reduced carbon contamination and high stoichiometric ratio of $[O_{InSn}]/1.5[In]+2[Sn]$ increase the work function. The surface stoichiometry of ITO is the dominant factor that controls the work function.

Acknowledgements. Support of this research by the Research Committee of Hong Kong Baptist University under Grant♯ FRG/98-99/II-71 is gratefully acknowledged. We would like to thank Professor Ho Wei for helpful discussions.

References

1. C.W. Tang, S.A. VanSlyke: Appl. Phys. Lett. **51**, 913 (1987)
2. N.C. Greenham, S.C. Moratti, D.D.C. Bradley, R.H. Friend, A.B. Holmes: Nature **365**, 629 (1993)
3. I.D. Parker: J. Appl. Phys. **75**, 1656 (1994)
4. Y. Yang, E. Westerweele, C. Zhang, P. Smith, A.J. Heeger: J. Appl. Phys. **77**, 694 (1995)
5. F. Steuber, J. Staudigel, M. Stössel, J. Simmerer, A. Winnacker: Appl. Phys. Lett. **74**, 3558 (1999)
6. C.C. Wu, C.I. Wu, J.C. Sturm, A. Kahn: Appl. Phys. Lett. **70**, 1348 (1997)
7. S.K. So, W.K. Choi, C.H. Cheng, L.M. Leung, C.F. Kwong: Appl. Phys. A **68**, 477 (1999)
8. F. Nüesch, L.J. Rothberg, E.W. Forsythe, Q. Toan Le, Y. Gao: Appl. Phys. Lett. **74**, 880 (1999)
9. A. Gyoutpku, S. Hara, T. Komatsu, M. Shihama, H. Iwanaga, K. Sakanoue: Synth. Met. **91**, 73 (1997)
10. M.G. Mason, L.S. Hung, C.W. Tang, S.T. Lee, K.W. Wong, M. Wang: J. Appl. Phys. **86**, 1688 (1999)
11. K. Sugiyama, H. Ishii, Y. Ouchi, K. Seki: J. Appl. Phys. **87**, 295 (2000)
12. I. Lindau, W.E. Spicer: J. Electron. Spectrosc. **3**, 409 (1974)
13. C.J. Powell: Surf. Sci. **44**, 29 (1974)
14. Y. Park, V. Choong, Y. Gao, B.R. Hsieh, C.W. Tang: Appl. Phys. Lett. **68**, 2699 (1996)
15. J.C.C. Fan, J.B. Goodenough: J. Appl. Phys. **48**, 3524 (1977)
16. R.B.H. Tahar, T. Ban, Y. Ohya, Y. Takahashi: J. Appl. Phys. **83**, 2631 (1998)
17. J.C.C. Fan, F.J. Bachner: J. Electrochem. Soc. **122**, 1719 (1975)
18. W.R. Salaneck, N. Johansson, K.Z. Xing, F. Cacialli, R.H. Friend, G. Beamson, D.T. Clark: Synth. Met. **92**, 207 (1998)